plants

MDPI

Article

Photosynthetic Gains in Super-Nodulating Mutants of *Medicago truncatula* under Elevated Atmospheric CO_2 Conditions

Rose Y. Zhang [1], Baxter Massey [1], Ulrike Mathesius [1] and Victoria C. Clarke [1,2,*]

[1] Research School of Biology, Australian National University, Canberra, ACT 2601, Australia
[2] Tasmanian Institute of Agriculture, University of Tasmania, Sandy Bay, TAS 7005, Australia
* Correspondence: tory.clarke@utas.edu.au

Abstract: Legumes are generally considered to be more responsive to elevated CO_2 (eCO_2) conditions due to the benefits provided by symbiotic nitrogen fixation. In response to high carbohydrate demand from nodules, legumes display autoregulation of nodulation (AON) to restrict nodules to the minimum number necessary to sustain nitrogen supply under current photosynthetic levels. AON mutants super-nodulate and typically grow smaller than wild-type plants under ambient CO_2. Here, we show that AON super-nodulating mutants have substantially higher biomass under eCO_2 conditions, which is sustained through increased photosynthetic investment. We examined photosynthetic and physiological traits across super-nodulating *rdn1-1* (Root Determined Nodulation) and *sunn4* (Super Numeric Nodules) and non-nodulating *nfp1* (Nod Factor Perception) *Medicago truncatula* mutants. Under eCO_2 conditions, super-nodulating plants exhibited increased rates of carboxylation (V_{cmax}) and electron transport (J) relative to wild-type and non-nodulating counterparts. The substantially higher rate of CO_2 assimilation in eCO_2-grown *sunn4* super-nodulating plants was sustained through increased production of key photosynthetic enzymes, including Rieske FeS. We hypothesize that AON mutants are carbon-limited and can perform better at eCO_2 through improved photosynthesis. Nodulating legumes, especially those with higher nitrogen fixation capability, are likely to out-perform non-nodulating plants under future CO_2 conditions and will be important tools for understanding carbon and nitrogen partitioning under eCO_2 conditions and future crop improvements.

Keywords: symbiosis; nitrogen; photosynthesis; elevated CO_2; super-nodulating mutants; *Medicago truncatula*

check for updates

Citation: Zhang, R.Y.; Massey, B.; Mathesius, U.; Clarke, V.C. Photosynthetic Gains in Super-Nodulating Mutants of *Medicago truncatula* under Elevated Atmospheric CO_2 Conditions. *Plants* **2023**, *12*, 441. https://doi.org/10.3390/plants12030441

Academic Editors: Xiaoming Xu and Haiyan Xiong

Received: 2 December 2022
Revised: 9 January 2023
Accepted: 16 January 2023
Published: 18 January 2023

Copyright: © 2023 by the authors. Licensee MDPI, Basel, Switzerland. This article is an open access article distributed under the terms and conditions of the Creative Commons Attribution (CC BY) license (https://creativecommons.org/licenses/by/4.0/).

1. Introduction

As atmospheric carbon dioxide (CO_2) levels continue to rise [1], plant productivity and crop yields will be impacted. As the primary photosynthetic substrate, elevated CO_2 (eCO_2) levels are anticipated to alter photosynthetic efficiency, as well as having potentially broader influences on developmental and physiological processes. The eCO_2 conditions reduce the frequency of photorespiration, enhancing photosynthetic rates and reducing respiratory costs [2]. This enhanced photosynthesis translates into positive growth responses for C_3 plants, with an average 20% increase in above-ground dry matter production under higher CO_2 concentrations [3]. Accordingly, C_3 crop species exhibit a 17% increase in yield under eCO_2, with cotton yields even increasing by over 40% [3]. While such yield responses may seem promising, high CO_2 concentrations produce grains with lower protein and amino acid content when compared to ambient-grown grains [4]. If crop plants are unable to maintain optimal carbon:nitrogen (C:N) ratios under eCO_2, the cost of reduced nutritional quality will outweigh the benefits of increased grain yield.

Long-term eCO_2 conditions tend to induce a characteristic photosynthetic acclimation response, where the overall benefit of eCO_2 becomes reduced due to the downregulation

of photosynthesis. This acclimation effect is most commonly observed through declines in the maximum carboxylation rate of Rubisco (V_{cmax}), as well as the maximum electron transport rate contributing to RuBP regeneration (J) [5]. There are two major hypotheses surrounding this acclimation or downregulation response [6], both of which are associated with the sensitivity of Rubisco to CO_2 and nitrogen (N) availability [7]. The "sink limitation" hypothesis suggests that greater carbon assimilation under eCO_2 increases carbohydrate concentration in leaves, resulting in the downregulation of photosynthetic enzyme synthesis. On the other hand, the "nitrogen limitation" hypothesis instead postulates that photosynthetic acclimation arises from nutrient, specifically nitrogen, limitation under greater carbon assimilation. Indeed, C_3 plants demonstrate significantly lower tissue %N when grown with eCO_2 compared with ambient CO_2 (aCO_2) conditions [8].

Studies indicate that in comparison with non-legumes, legumes experience greater stimulation of photosynthesis under eCO_2 [3,9]. The key factor contributing to this response is the development of symbiotic nitrogen fixation (SNF) in legumes. SNF allows legumes to obtain biologically available forms of nitrogen from nitrogen-fixing bacteria known as rhizobia. During the initiation of SNF, legumes secrete rhizobia-specific flavonoids from their roots. These compounds activate the expression of rhizobial *Nod* genes, followed by Nod factor perception by the host legume, bacterial infection, and nodule development [10]. Once rhizobia successfully infect the host legume, they differentiate into bacteroids and inhabit a specialized root structure known as the nodule. In exchange for bio-available nitrogen compounds, the host legume provides the rhizobia with carbohydrates in the form of malate and other organic acids [11].

Not only does SNF provide legumes with a greater pool of available nitrogen, it also acts as a sink for carbohydrates assimilated in the leaves. Under eCO_2 conditions, SNF compensates for cellular reductions in N while preventing the downregulation of key photosynthetic enzymes including Rubisco by acting as a carbon sink. Substantial experimental evidence supports the enhanced performance of nodulating legumes under eCO_2 [12,13]. Some studies report greater nodule numbers and nodule biomass under eCO_2 [7], while others observe far higher levels of total leaf N, specific leaf area (SLA), and harvestable biomass [14,15].

The responsiveness and sensitivity of nodulation to eCO_2 suggests that photosynthesis and nodulation are closely regulated and interdependent. At a fundamental level, photosynthetic machinery imposes a heavy nitrogen cost upon plants, with chloroplasts composing 75% of average C_3 leaf nitrogen [16]. Rubisco alone makes up 40% of soluble protein and 20% of leaf nitrogen in C_3 leaves [16]. Likewise, nodulation imposes a heavy carbon cost upon plants, with the maintenance of active nodules estimated to require at least 6 g of carbon per gram of nitrogen obtained, although this depends on the environmental conditions and efficiency of the SNF [17,18]. To control the high carbohydrate demand of nodules, legumes display autoregulation of nodulation (AON) to restrict nodules to the minimum number needed to sustain nitrogen supply under current photosynthetic levels [19].

AON has been hypothesized to act as a systemic signaling mechanism, requiring a complex signal transduction process between the roots and the shoots [20,21]. In the model legume *Medicago truncatula*, the initial infection of rhizobia into the roots induces the local production of CLE12 and CLE13 peptides [22,23]. The CLE12 peptide is activated by tri-arabinosylation in the root by the enzyme RDN (Root Determined Nodulation) [20,24]. Both peptides are then transported into the shoot via the xylem, where they are perceived by the leucine-rich repeat receptor kinase (LRR-RK) SUNN (Super Numeric Nodules) [25]. Disruption to various components of this signaling mechanism can result in abnormal nodule development. Super-nodulating legumes have a deficient AON pathway and are unable to regulate their nodule numbers [19]. Instead, they produce excessive numbers of nodules at high physiological cost to the plant. At ambient CO_2, the *M. truncatula* AON mutants *sunn4* and *rdn1-1* are characterized by numerous small nodules, lower biomass but higher %N in shoot and root tissues, at least at low external nitrogen supply [26], similar

to AON mutants in other species [27]. On the other hand, non-nodulating legumes are defective in the processes required to initiate rhizobial symbiosis, preventing them from exhibiting SNF.

In this study, we assessed various phenotypic traits of the model legume *Medicago truncatula* across wild-type (cultivar A17), super-nodulating mutants *rdn1-1* and *sunn4*, and the non-nodulating mutant *nfp1* [28] under two different CO_2 treatments: ambient (500 µmol mol^{-1} CO_2) and elevated (1000 µmol mol^{-1} CO_2). We assessed CO_2 assimilation rate, chlorophyll fluorescence and plant physiology parameters alongside levels of the photosynthetic enzymes to elucidate the extent of nitrogen allocation toward photosynthetic machinery in AON mutants.

2. Results

2.1. Super-Nodulating Plants Are More Photosynthetically Responsive to Elevated CO_2

CO_2 response curves revealed similar rates of CO_2 assimilation in ambient-grown (aCO_2) *rdn1-1* and *sunn4* super-nodulating mutants relative to ambient-grown wild-type plants (Figure 1A). In contrast, *rdn1-1* and *sunn4* mutants exhibited significantly higher CO_2 assimilation rates than wild-type plants when grown under elevated CO_2 conditions (eCO_2), while non-nodulating *nfp1* plants exhibited the lowest CO_2 assimilation rates across both CO_2 treatments (Figure 1B). Both measured and model-derived estimates of maximum electron transport (J) support this trend, with eCO_2 *rdn1-1* and *sunn4* mutants displaying significantly higher J estimates relative to eCO_2 wild-type and *nfp1* plants (Figure 2B & Table 1). When grown under eCO_2, *rdn1-1* and *sunn4* mutants also displayed increased maximum electron transport and maximum Rubisco activity (V_{cmax}) (Figure 2A) when compared with their ambient-grown counterparts.

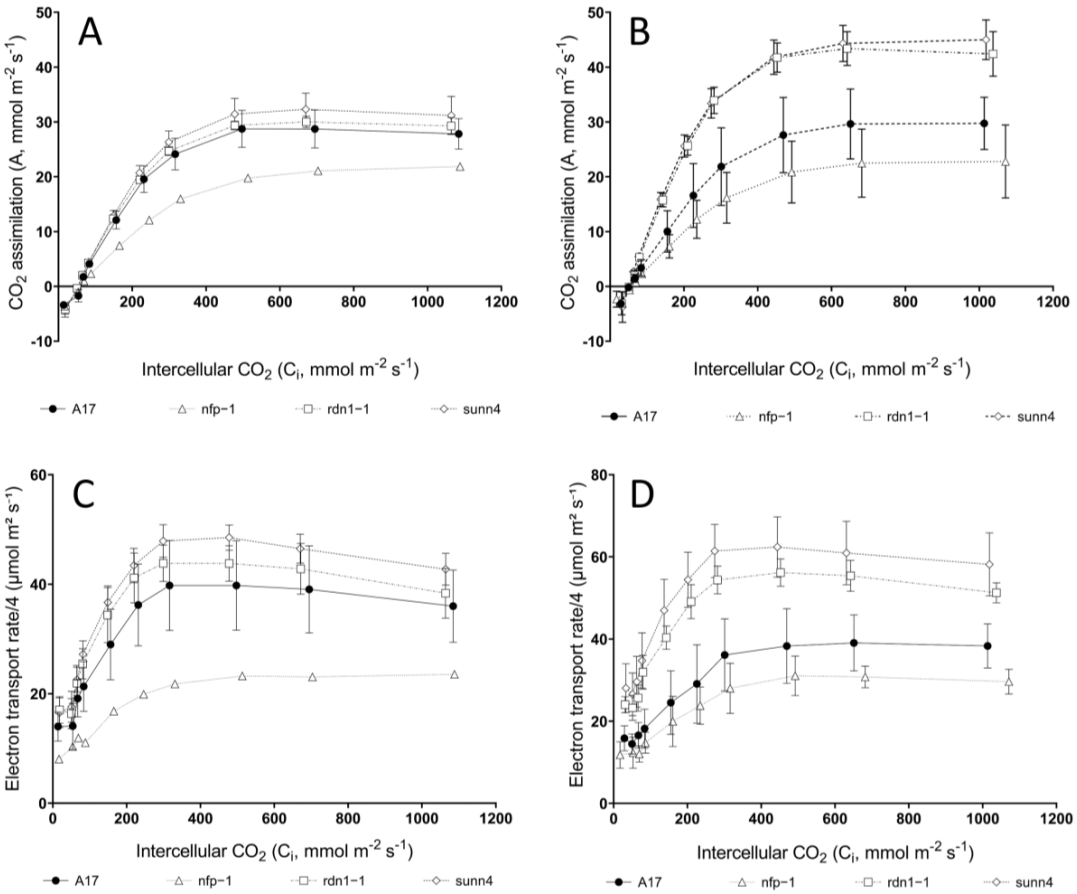


Figure 1. CO_2 responses curves (**A**,**B**) and electron transport rates (**C**,**D**) of *Medicago truncatula* nodulation mutants (open symbols) were comparable to wild-type plants (solid symbol) when grown

under ambient CO_2 levels (**A**,**C**), but differed significantly under elevated CO_2 levels (**B**,**D**). Measurements were taken at 25 °C and 21% O_2. Error bars represent standard deviation; see footnotes of Table 1 for sample sizes.

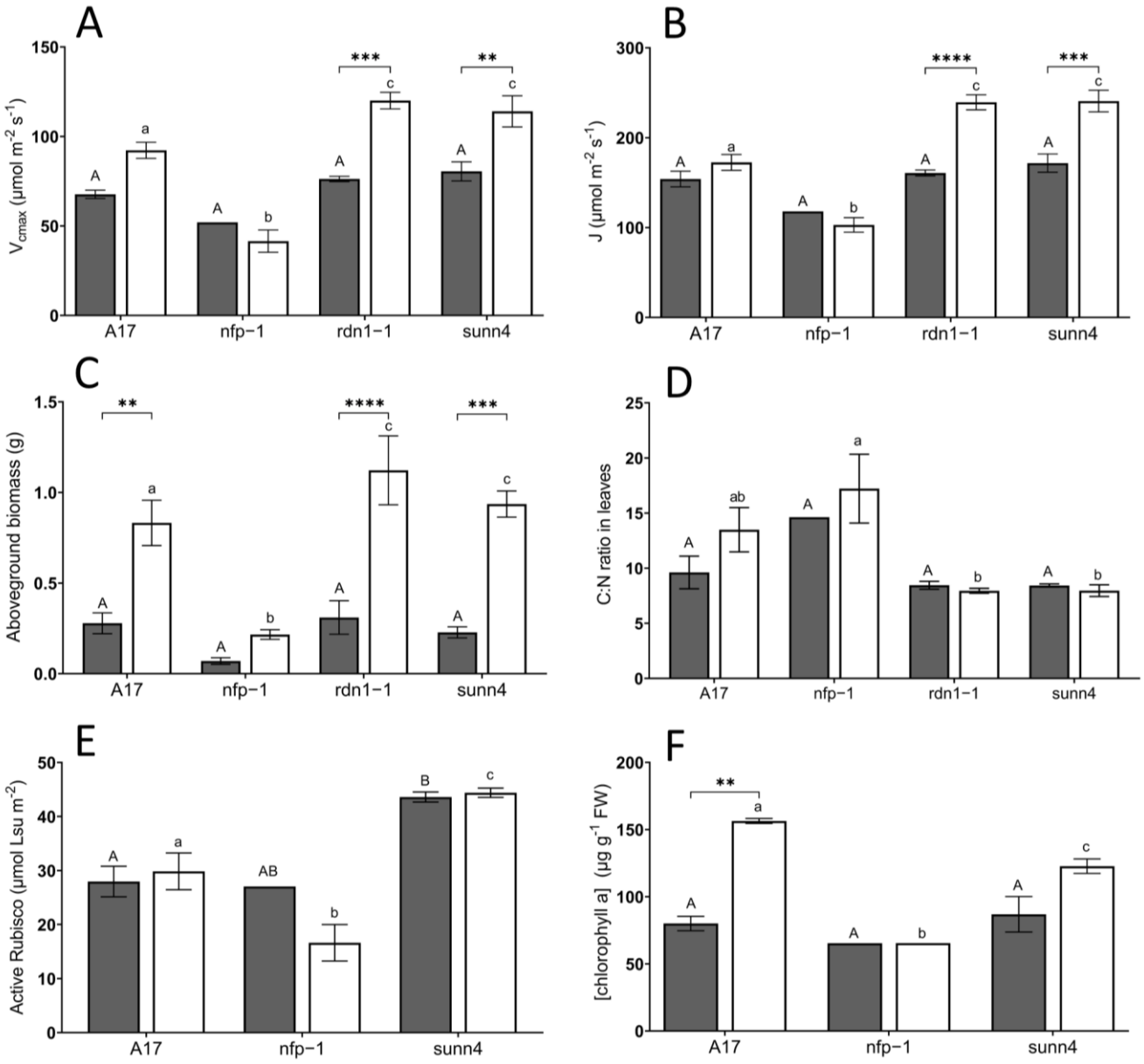


Figure 2. Comparisons of (**A**) maximum Rubisco activity, V_{cmax}, (**B**) maximum electron transport, J, (**C**) above-ground biomass, (**D**) carbon/nitrogen ratio, (**E**) active Rubisco content, and (**F**) chlorophyll A concentration in leaves of *Medicago truncatula* lines grown at ambient (aCO_2, dark grey bars) and elevated (eCO_2, white bars) conditions. Error bars represent standard error; see footnotes of Table 1 for sample sizes. Asterisks indicate level of statistical significance (** = $p < 0.01$, *** = $p < 0.001$, **** = $p < 0.0001$) in pairwise differences between CO_2 treatments. Uppercase letters describe significant groupings at ambient CO_2 levels while lowercase letters describe significant groups at elevated CO_2 levels; values which do not share a common letter display statistical significance from each other.

Table 1. Various phenotypic traits in wild-type (A17), super-nodulating (*rdn1-1* and *sunn4*) and non-nodulating (*nfp1*) *Medicago truncatula* plants grown at ambient (aCO_2, dark grey cells) and elevated (eCO_2, white cells) conditions. Uncertainty (±) is derived from standard error; cells with a dash (-) were not quantified for the relevant trait. Values in bold indicate statistically significant ($p < 0.05$) pairwise differences between CO_2 treatments. Uppercase letters describe significant groupings at ambient CO_2 levels while lowercase letters describe significant groups at elevated CO_2 levels; values within a row that do not share a common letter display statistical significance ($p < 0.05$) from each other. * $n = 1$ for aCO_2 *nfp1*; $n = 3$ for aCO_2 A17, $n = 4$ for eCO_2 A17, eCO_2 *nfp1*, eCO_2 *sunn4*, aCO_2 *rdn1-1*, aCO_2 *sunn4*; $n = 5$ for eCO_2 *rdn1-1*. # $n = 1$ for aCO_2 *nfp1*, eCO_2 *nfp1*; $n = 3$ for aCO_2 A17, aCO_2 *sunn4*, eCO_2 A17, eCO_2 *sunn4*. † $n = 5$ for all treatments. ‡ $n = 1$ for aCO_2 *nfp1*, eCO_2 *nfp1*; $n = 3$ for aCO_2 A17, aCO_2 *sunn4*, eCO_2 A17, eCO_2 *sunn4*.

	Genotype and Treatment							
	aCO_2 A17	**eCO_2 A17**	**aCO_2 *nfp1***	**eCO_2 *nfp1***	**aCO_2 *rdn1-1***	**eCO_2 *rdn1-1***	**aCO_2 *sunn4***	**eCO_2 *sunn4***
V_{cmax} (μmol m^{-2} s^{-1}) *	68 ± 2.6 ^{A}	92 ± 4.4 ^{a}	52 ^{A}	41 ± 6.1 ^{b}	76 ± 1.4 ^{A}	**120 ± 4.8 ^{c}**	81 ± 5.3 ^{A}	**114 ± 8.6 ^{c}**
J (μmol m^{-2} s^{-1}) *	154 ± 8.8 ^{A}	173 ± 8.9 ^{a}	118 ^{A}	103 ± 8.0 ^{b}	161 ± 3.2 ^{A}	**239 ± 12 ^{c}**	172 ± 10 ^{A}	**154 ± 8.8 ^{c}**
Stomatal conductance at 400 ppm (mol m^{-2} s^{-1}) *	0.52 ± 0.02 ^{A}	0.41 ± 0.06 ^{a}	0.38 ^{A}	0.32 ± 0.05 ^{a}	0.45 ± 0.02 ^{A}	0.51 ± 0.08 ^{a}	0.47 ± 0.04 ^{A}	0.44 ± 0.04 ^{a}
Electron transport rate/4 at 400 ppm (μmol m^{-2} s^{-1}) *	42 ± 4.1 ^{A}	37 ± 4.2 ^{a}	23 ^{AB}	29 ± 4.3 ^{a}	48 ± 2.4 ^{AC}	59 ± 1.8 ^{b}	51 ± 1.5 ^{AC}	64 ± 3.0 ^{b}
Active Rubisco content (μmol LSU m^{-2}) #	28 ± 2.8 ^{A}	30 ± 3.4 ^{a}	27 ^{AB}	17 ± 3.4 ^{b}	-	-	44 ± 0.94 ^{B}	44 ± 0.86 ^{c}
[Chlorophyll A] (μg g^{-1} FW) #	80 ± 5.3 ^{A}	**156 ± 1.8 ^{a}**	63 ^{A}	65 ^{b}	-	-	87 ± 13 ^{A}	123 ± 5.4 ^{c}
Specific leaf area (m^{-2} g) *	0.035 ± 0.003 ^{A}	0.021 ± 0.003 ^{a}	0.027 ^{A}	0.025 ± 0.003 ^{a}	0.026 ± 0.004 ^{A}	0.029 ± 0.002 ^{a}	0.030 ± 0.002 ^{A}	0.023 ± 0.004 ^{a}
Above-ground biomass (g) †	0.28 ± 0.058 ^{A}	**0.83 ± 0.125 ^{a}**	0.070 ± 0.018 ^{A}	0.22 ± 0.027 ^{b}	0.31 ± 0.093 ^{A}	**1.12 ± 0.19 ^{c}**	0.23 ± 0.031 ^{A}	**0.94 ± 0.072 ^{c}**
Relative Rieske protein content ‡	0.72 ± 0.15 ^{A}	0.83 ± 0.068 ^{a}	-	0.46 ^{a}	-	-	0.89 ± 0.03 ^{A}	1.38 ± 0.10 ^{b}
Relative Rubisco protein content ‡	0.70 ± 0.16 ^{A}	0.73 ± 0.077 ^{a}	-	0.48 ^{a}	-	-	0.75 ± 0.071 ^{A}	1.05 ± 0.11 ^{a}
%N in leaves *	4.57 ± 0.67 ^{A}	3.05 ± 0.46 ^{a}	2.80 ^{A}	2.34 ± 0.44 ^{a}	5.18 ± 0.21 ^{A}	5.36 ± 0.15 ^{b}	5.23 ± 0.08 ^{A}	5.38 ± 0.36 ^{b}
%C in leaves *	43.9 ± 1.3 ^{A}	**41.1 ± 0.3 ^{ab}**	41.0 ^{A}	40.3 ± 0.5 ^{a}	43.7 ± 0.3 ^{A}	42.7 ± 0.5 ^{b}	44.1 ± 0.4 ^{A}	42.9 ± 0.4 ^{b}
C:N ratio in leaves *	9.61 ± 1.48 ^{A}	13.5 ± 2.0 ^{ab}	14.6 ^{A}	17.2 ± 3.1 ^{a}	8.45 ± 0.36 ^{A}	7.95 ± 0.22 ^{b}	8.43 ± 0.14 ^{A}	7.96 ± 0.53 ^{b}

Western blot analysis was performed on a subset of samples grown at both CO_2 concentrations. The *sunn4* super-nodulating mutant was not significantly different to wild-type in the amount of rubisco small subunit protein detected, under both CO_2 conditions (Figure 3B). Total rubisco content (measured by CABP-binding assay) was higher in *sunn4* mutants than wild-type controls at both CO_2 concentrations but was not significantly different between CO_2 concentrations within any genotype (Figure 2C). The relative Rieske protein content, as determined by western blot, of eCO_2 *sunn4* mutants was almost two-fold higher than in eCO_2 wild-type plants, and three-fold higher than eCO_2 *nfp1* mutants (Figure 3A). Across all nodulation genotypes, plants with higher Rubisco and Rieske content tend to exhibit correspondingly higher rates of maximum Rubisco activity (V_{cmax}) and maximum electron transport (J), respectively (Figure 4A,B). Active Rubisco content also shows positive affiliation with increased leaf %N (Figure 4C).

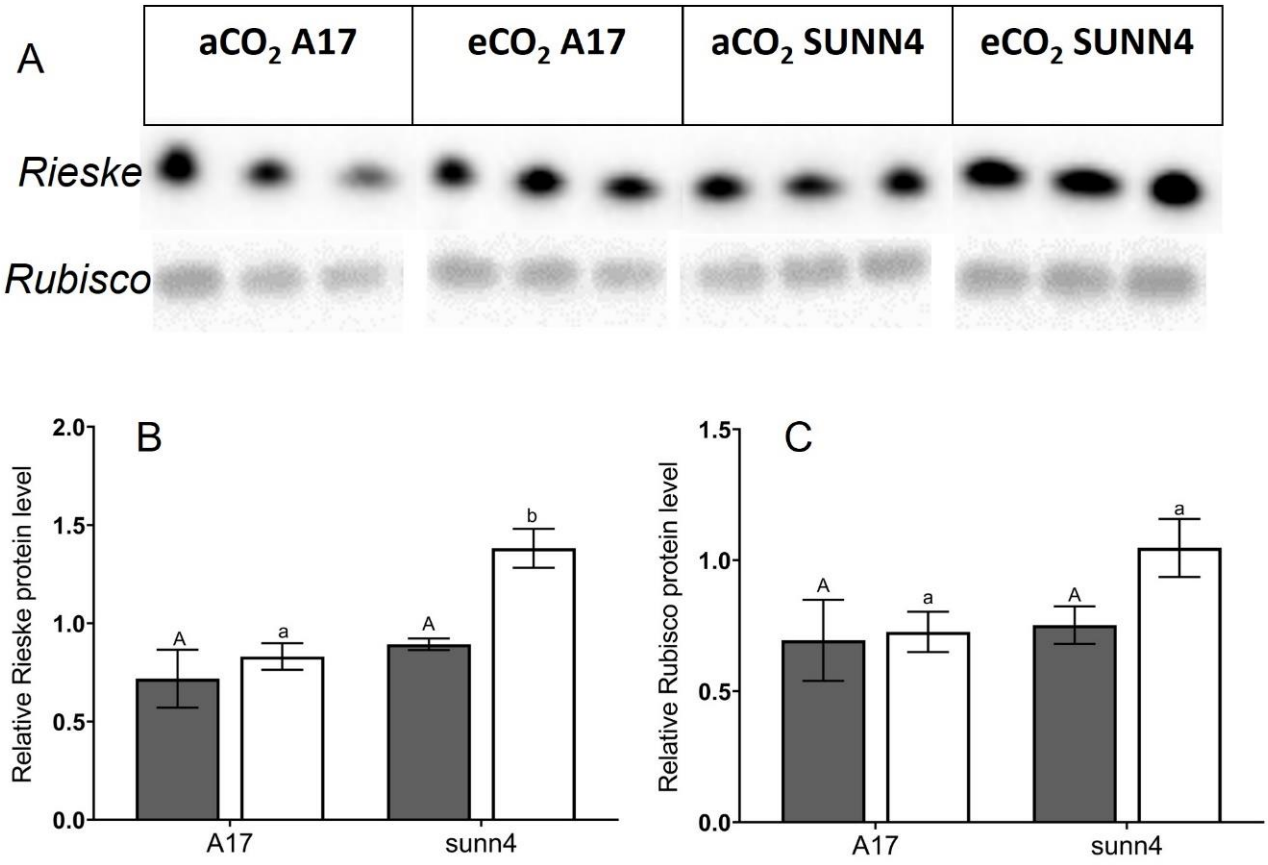


Figure 3. (**A**) Western Blot analysis of Rieske and Rubisco protein content in wild-type and *sunn-4* super-nodulating *Medicago truncatula* lines grown at ambient (aCO_2, dark grey bars) and elevated (eCO_2, white bars) conditions. (**B**) *Medicago truncatula sunn4* super-nodulating mutant displays significantly higher relative Rieske protein levels than wild-type and non-nodulating plants under elevated CO_2 levels (white bars), but not under ambient CO_2 levels (dark grey bars). (**C**) The relative Rubisco protein level of the *Medicago truncatula sunn4* super-nodulating mutant do not differ significantly from wild-type plants under both ambient (dark grey bars) and elevated CO_2 levels (white bars). Error bars represent standard error; see footnotes of Table 1 for sample sizes. Uppercase letters describe significant groupings at ambient CO_2 levels while lowercase letters describe significant groups at elevated CO_2 levels; values which do not share a common letter display statistical significance from each other.

In contrast with generally observed improvements in photosynthetic activity in super-nodulating mutants under eCO_2, wild-type plants grown under eCO_2 conditions displayed significantly higher concentrations of chlorophyll A than super-nodulating plants (Figure 2D). Stomatal conductance was largely unresponsive to CO_2 concentration and plant genotype, with comparable values across all treatments (Table 1).

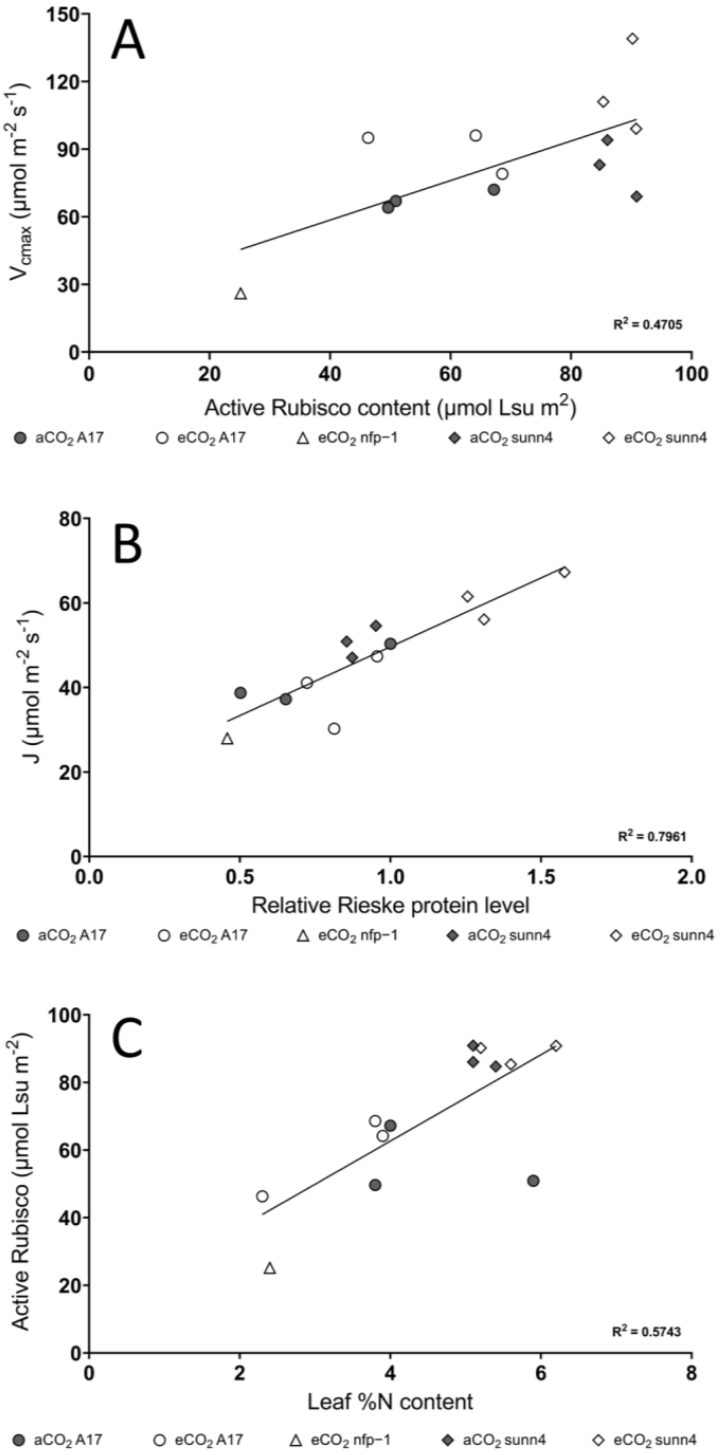


Figure 4. The relationship between (**A**) active Rubisco content and V_{cmax}, (**B**) relative Rieske protein level and (J), (**C**) leaf %N content and active Rubisco content in *Medicago truncatula* wild-type plants (A17, circles), a super-nodulating mutant *sunn4* (diamonds) and the non-nodulating mutant *nfp-1* (triangles) at ambient CO_2 (aCO_2, dark markers) and elevated CO_2 (eCO_2, white markers).

2.2. Super-Nodulating Plants have Increased Biomass and Leaf Nitrogen Content under Elevated CO_2 Conditions

Wild-type, *rdn1-1,* and *sunn4* plants exhibited a significant three-to-four-fold increase in above-ground biomass (AGB) when grown under elevated CO_2 conditions compared to ambient CO_2 conditions (Figure 2E). Within the elevated CO_2 treatment, *nfp1* mutants had

significantly lower AGB than wild-type plants, while the AGB of *rdn1-1* and *sunn4* mutants was significantly higher (10–35% increase) than wild-type plants.

Under both CO_2 conditions, *nfp1* plants exhibited higher leaf carbon:nitrogen (C:N) ratios than super-nodulating plants, with this difference being significant at eCO_2 (Figure 2F).

Interestingly, the carbon content (%C) in leaves of wild-type plants experienced a significant decline when grown at eCO_2 conditions, while neither *nfp1* nor super-nodulating plants demonstrating any shift in carbon content under eCO_2 (Table 1). At eCO_2, %N in leaves was also significantly increased in super-nodulating plants compared to the wild-type control (Table 1).

3. Discussion

This study assessed carbon and nitrogen assimilation in super-nodulating (*rdn1-1* and *sunn4*) and non-nodulating (*nfp1*) mutants of *Medicago truncatula* under ambient and elevated CO_2 conditions to better understand the role of symbiotic nitrogen fixation (SNF) in mediating photosynthesis under eCO_2 levels.

Wild-type plants, with the ability to autoregulate nodule number, were expected to increase their biomass production, N fixation, and N assimilation under high CO_2 as a result of a greater carbon supply to the nodules [29]. We found that biomass and chlorophyll content were increased under eCO_2 conditions (Figure 2, Table 1). We hypothesized that this response to elevated CO_2 would be modulated by higher CO_2 assimilation rate and potentially increased N allocation toward photosynthetic machinery, but while trending higher, these differences were not significant in wild-type plants between the two CO_2 conditions (Table 1). Leaf N and carbon (C) content, however, were reduced in the leaves of wild-type plants grown under eCO_2, with the C:N ratio trending higher but not significantly different (Table 1). This suggests that despite having increased N availability due to SNF, wild-type *Medicago* plants may still be N limited under eCO_2 conditions and are not able to effectively re-direct additional C assimilated in photosynthesis to SNF. Leaf ^{15}N content (a proxy for SNF) measurements were unreliable in this study so N fixation impacts could not be determined (data not shown).

The super-nodulating *rdn1-1* and *sunn4* mutants were expected to perform sub-optimally at ambient CO_2 levels due to the high C cost of super-nodulation, though we observed no significant decrease in photosynthetic or physiological traits compared to wild-type plants at ambient CO_2 (Table 1). This may be due to the ambient CO_2 level in our growth chambers being at 500 µmol mol^{-1} CO_2, enabling the super-nodulators to maximize SNF. Previous analyses of *sunn4* and *rdn1-1* mutants in *Medicago* also did not find significant decreases in shoot biomass at ambient (400 µmol mol^{-1} CO_2) levels compared to the A17 wild-type plant, with *rdn1-1* even having a higher shoot biomass than wild-type plants at 550 µmol mol^{-1} CO_2 [30]. At elevated CO_2 levels, however, the *sunn4* and *rdn1-1* super-nodulating mutants had substantially increased photosynthetic activity and biomass accumulation. *Sunn4* and *rdn1-1* had significantly increased maximum carboxylation (V_{cmax}) and electron transport rate (J) when grown at eCO_2 compared to aCO_2, which was not observed in wild-type plants (Figure 2A,B).

Across all nodulation genotypes, plants with higher Rubisco and Rieske content also had correspondingly higher rates of maximum Rubisco activity (V_{cmax}) and maximum electron transport (J), respectively (Figure 4A,B). The substantially higher rate of CO_2 assimilation in eCO_2-grown *rdn1-1* and *sunn4* plants relative to wild-type plants is sustained by increased production of key photosynthetic enzymes, with the *sunn4* super-nodulating mutant having significantly increased Rieske protein levels compared to the wild-type control (Figure 3B). Rieske FeS (PetC) forms one of four major subunits contained within the Cytochrome b_6f (Cytb_6f) monomer, and in its dimeric form, Cytb_6f forms one of the major protein complexes within the electron transport chain of C_3 plants [31]. Increased Rieske expression has been associated with an upregulation of Cytb_6f as well as improved CO_2 assimilation [32], making it a useful biochemical proxy for electron transport rate.

The *sunn4* super-nodulating mutant also had increased total Rubisco content at both aCO_2 and eCO_2 compared to wild-type controls (Figure 2E). Rubisco is composed of eight small and eight large subunits, and is the major photosynthetic enzyme, responsible for catalyzing the reaction of CO_2 with ribulose 1,5-bisphosphate (RuBP) during the carbon assimilation process [33]. *Rdn1-1* samples were not able to be assessed for Rubisco or Rieske content, but it would be expected they would also have increased levels similar to *sunn4* due to their increased carboxylation and electron transport rates as determined through CO_2 response curves (Figure 2A,B). It is important to note, however, that the wild-type control (A17) in this experiment has the same background as *rdn1-1* (Jemalong A17), while the *sunn4* line has a related, but different, background (Jemalong J5). While *rdn1* and *sunn4* had similar physiological responses to eCO_2, and there are no reported physiological differences between the lines [25], it is possible that the biochemical differences between *sunn4* and WT A17 plants may be influenced by differences in their background genotype.

This upregulation of photosynthetic enzymes and CO_2 assimilation is unique to the super-nodulating genotype and lies in contrast to widely reported acclimation responses to eCO_2 across nodulating legumes that exhibit autoregulation of nodulation (AON). A meta-analysis by Ainsworth and Long [3] evaluated over 15 pairwise comparisons across three legume species grown at ambient and elevated CO_2 levels, and found an average decline in V_{cmax} and J by ~6% and ~13%, respectively. Likewise, when grown under seven different CO_2 concentrations, soybean exhibit dramatically lower V_{cmax} and J beyond optimal CO_2 concentrations of 400–600 μmol mol^{-1} CO_2 [34]. Calculations based on legumes grown under free-air CO_2 enrichment (FACE) experiments also suggest a 10% reduction in leaf rubisco content between current and elevated CO_2 concentrations [5]. As such, super-nodulating mutants of *M. truncatula* appear to be capable of overcoming eCO_2-induced photosynthetic acclimation.

The non-nodulating *nfp1* mutant is entirely unable to form nodules and had similar physiology to non-legumes under high CO_2, with substantial N limitation resulting in reduced photosynthetic performance and decreased biomass (Table 1). Non-nodulating legumes, such as *nfp1,* display higher C:N ratios under eCO_2 due to N limitation [4,35]. In this study, while C:N ratios tended higher in the non-nodulating *nfp1* mutant, this difference was not significant, likely due to the reduced sample replication possible in these very small plants (Figure 2D, Table 1). The super-nodulating *rdn1-1* and *sunn4* mutants were observed to maintain relatively constant C:N ratios, however (Figure 2D, Table 1). This unique capacity for *rdn1-1* and *sunn4* mutants to enhance CO_2 assimilation rate while maintaining C:N ratios arises from the greater N availability provided by super-nodulation [30]. Active rubisco content also shows positive affiliation with increased leaf %N across the lines (Figure 4C). With Rubisco accounting for 20% of leaf nitrogen content in C_3 plants [16], this correlation provides further support that additional N obtained through SNF in the super-nodulating legumes is able to be invested in photosynthesis

In this study, the impact of greater N assimilation on photosynthetic enzyme content could not be conclusively established through analyzing the portion of N assimilated through SNF, as root $\delta^{15}N$ values may have been contaminated from the presence of potting vermiculite (Stuart-Williams, personal communication). Where possible, the cultivation of legumes in hydroponic rather than soil medium may allow for more extensive and reliable ^{15}N quantification, and this approach would also make nodules more readily accessible for morphological or phenotypic assays. ^{13}C analysis of C assimilation integration data was also not possible in this study due to the differing ^{13}C signature of the eCO_2 air supplementation compared to ambient CO_2.

The physiological outcome of enhanced C and N assimilation in super-nodulating legumes is evident in the significant above-ground biomass accumulation in *rdn1-1* and *sunn4* plants at eCO_2 conditions (Figure 2C), which has also been observed in *rdn1-1* previously [30], but not in soybean super-nodulating mutants grown at high light and/or CO_2 [36,37]. While Ainsworth, Davey [38] report greater shoot dry weight (SDW) improvement in non-nodulating soybeans (76% improvement) compared to nodulating soybeans

(28% improvement), this study reports greater relative AGB increase in super-nodulating and wild-type *M. truncatula* plants compared to non-nodulating *nfp1* plants. This discrepancy may arise from a greater rhizobial carbon demand in soybeans compared to *M. truncatula* or suggests the potential for different C and N allocation regimes between legume species. Nodulating soybean plants may increase C allocation to seeds under eCO_2, while nodulating *M. truncatula* plants may instead prioritise shoot growth. Indeed, soybean seeds produced under elevated CO_2 conditions have been found to accumulate higher C and isoflavone content compared to seeds produced under ambient CO_2 conditions [39,40].

Across both ambient and elevated CO_2 conditions, *rdn1-1* and *sunn4* mutants performed comparably within all the phenotypic traits assessed in this study. This indistinguishability between *rdn1-1* and *sunn4* lies in contrast to results from Qiao, Miao [30], wherein eCO_2-grown *sunn4* mutants exhibited significantly reduced shoot and root biomass, as well as total N per plant, fixed N per plant, and fixed N per nodule when compared with eCO_2-grown *rdn1-1* mutants. Greater phenotypic differences between *rdn1-1* and *sunn4* would be expected given the distinct nodule responses that have been previously documented for these two super-nodulating mutants, with greater nodule mass and number in *sunn4* compared to *rdn1-1* mutants at ambient [26] and elevated CO_2 [30]. Differences in experimental design may account for this disparity, as Qiao et al. examined phenotypic responses in soil and under a CO_2 concentration of 300–850 μmol mol^{-1} CO_2, while CO_2 treatments in this study ranged from 500–1000 μmol mol^{-1} CO_2. Physiological responses in plants often exhibit a bell-shaped curve with respect to environmental variables such as CO_2 concentration [34], with comparisons between different points on the curve thus yielding different outcomes. In order to address this discrepancy, future studies could further elucidate subtle differences between *rdn1-1* and *sunn4* super-nodulating mutants through cultivation under a wider range of CO_2 concentrations.

Ultimately, through comparisons between *rdn1-1/sunn4*, wild-type, and *nfp1* plants, this study provides compelling evidence for the capacity of symbiotic nitrogen fixation to support greater photosynthetic assimilation under elevated CO_2 conditions. Under the elevated CO_2 conditions in this study (1000 μmol mol^{-1} CO_2), super-nodulating legumes were able to re-invest the additional N fixed through SNF back into photosynthesis to overcome C limitations. The ability of legumes to obtain a reliable source of N from SNF, and the ability of super-nodulating legumes to further enhance these benefits will inform efforts to providing reliable and nutritious crop yields under future elevated CO_2 conditions. Future field-based experiments, such as those conducted using FACE techniques, will be critical in determining whether presently observed improvements to photosynthesis and plant growth can be sustained in the absence of controlled laboratory conditions.

4. Materials and Methods

4.1. Plant Material

Medicago truncatula seeds of the wild type line Jemalong A17, the non-nodulation mutant *nfp1* [derived from A17, 28], the *sunn4* mutant [derived from the related genotype Jemalong J5, 25], and the *rdn1-1* mutant [derived from Jemalong A17, 20] were used. The *rdn1-1* mutant has a 103-kb deletion that includes *RDN1* as well as 17 other annotated genes [20]. So far, no obvious phenotypic differences have been reported between the wild type cultivars Jemalong A17 and Jemalong J5 [25].

Seeds were chemically scarified in concentrated H_2SO_4 for 3 min, thoroughly washed with water, and surface-sterilized in NaClO for 5 min before being washed in sterile Milli-Q water. After germination at 25 °C overnight, seedlings were sown in pots filled with vermiculite. One seedling was grown in each pot. Pots were arranged in a random block design with ten replicates (ten blocks within each growth room). Vermiculite was used because it contains little to no residual nitrogen, allowing nitrogen concentration to be externally controlled. A volume of 50 mL of nutrient solution (Fåhraeus Medium; composition (mg/L) of KH_2PO_4, 217; K_2SO_4, 74; $CaCl_2{\cdot}2H_2O$, 244; $MgSO_4{\cdot}7H_2O$, 122; NaB_4O_7, 1.6; $MnSO_4{\cdot}H_2O$, 6; $ZnSO_4{\cdot}7H_2O$, 8; $CuSO_4{\cdot}5H_2O$, 6; $CoCl_2$, 0.4; Na_2MoO_4,

0.4; $FeCl_3$, 0.6.) was provided to each pot every 3 days. Once a week, each pot also received 1 mL of 0.5 mM KNO_3 that was enriched with ^{15}N at 1% atom excess. This enriched the growth medium in ^{15}N, enhancing the difference in ^{15}N between soil-derived and atmosphere-derived nitrogen and allowing for estimation of nitrogen derived from atmospheric nitrogen [41].

Two weeks after germination, seedlings were inoculated with a cultured suspension of the *M. truncatula* symbiont *Sinorhizobium meliloti* strain 1022. The rhizobia were first grown on a plate of solid BBM agar [42] and then a single colony was picked and grown overnight in liquid BMM in a 50 mL Falcon tube. After 16 h, the optical density (OD) of the rhizobial suspension was measured with a spectrophotometer at 600 nm and adjusted to an OD_{600} of 0.1 to standardize rhizobial density. Each pot received 1 mL of this suspension.

4.2. Growth Conditions

From 2 weeks post-germination, plants were grown under controlled-environment conditions in two growth rooms (Controlled Environment Facility, ANU). The ambient CO_2 (aCO_2) growth chamber was maintained at ~500 µmol mol^{-1} CO_2 (it was not possible to maintain the CO_2 to a value closer to the current ambient CO_2 of 414 µmol mol^{-1} CO_2), while the elevated CO_2 (eCO_2) growth chamber was maintained at ~1000 µmol mol^{-1} CO_2 (average concentration over 24 h). Both chambers had 16 h:8 h light:dark cycles, with day temperatures of 23 °C, ~250 µE light intensity, and a set humidity of 60% (actual humidity levels varied between 50–70%).

4.3. Photosynthetic Activity

CO_2 response curves of carbon assimilation rate and chlorophyll fluorescence were measured together with a LI-6800 portable photosynthesis system (LI-COR Biosciences, Lincoln, NE, USA), at a leaf temperature of 25 °C, irradiance of 1500 µmol quanta m^{-2} s^{-1}, relative humidity of 55%, 21% O_2, and varying reference CO_2 concentrations (0, 50, 75, 100, 200, 300, 400, 600, 800, and 1200 µmol mol^{-1}). All measurements were taken from the youngest, fully expanded trifolate leaf on the longest shoot of 7-week-old plants. Each measured trifolate leaf was photographed alongside a reference ruler, and total leaf area was extracted using ImageJ Java 1.8.0_172 [43] to correct for leaf area within the LI-6800 chamber. Curves were analyzed to derive estimates of maximum Rubisco activity, V_{cmax}, and the rate of electron transport, J [44]. Fluorescence-based measurements of electron transport rate (ETR) are also considered equivalent to J when divided by four (J = ETR/4). Leaf discs were harvested from measured plants, oven-dried, and weighed to determine specific leaf area (SLA), and above-ground biomass (AGB) was determined from mature plants harvested at 9 weeks of age.

4.4. Biochemical Assays

For biochemical analysis of leaves, leaf discs of 0.353 cm^2 corresponding to the area where gas exchange was measured were collected and frozen immediately in liquid N_2. Active Rubisco content was estimated from leaf discs by the irreversible binding of [^{14}C]2-carboxy-D-arabinitol 1,5-bisphosphate to the fully carbamylated enzyme, as described by Ruuska et al. [45].

In order to isolate leaf proteins, protein extract derived from the active Rubisco assay was diluted into 4x SDS Sample buffer containing 0.25 M tris-HCl pH 6.8, 40% (*v/v*) glycerol, 8% SDS, 4% bromophenol blue, 0.5% betamercaptoethanol, and incubated at 95° C for 5 min. Samples were loaded on a leaf area basis and separated by polyacrylamide gel electrophoresis (Nu-PAGE 4–12% Bis-(2-hydroxyethyl)-amine-tris(hydroxymethyl)-methane (Bis-Tris) gel, Invitrogen, Life Technologies Corporation, Carlsbad, CA) in running buffer (pH 7.3) containing 50 mM 2-(N-morpholino)ethanesulfonic acid, 50 mM trisaminomethane, 0.1% sodium dodecylsulfate (*w/v*), and 20 mM ethylenediaminetetraacetic acid. Proteins were transferred to a nitrocellulose membrane and probed with antibodies against Rieske FeS protein (Agrisera cat. no. AS08330, Vännäs, Sweden) at 1:3000 dilution, and Rubisco small

subunit protein (Agrisera cat. no. AS07259, Vännäs, Sweden) at 1:10,000 dilution. Quantification of Western blots was performed with Image Lab software (Biorad Laboratories, Hercules, CA, USA).

Leaf chlorophyll was extracted in 80% acetone and sample absorbance was determined with an Agilent Cary 60 UV-Vis spectrophotometer (Agilent Technologies, USA) at 663.2 nm and 646.8 nm against an 80% acetone blank. Chlorophyll A content was determined from sample absorbance according to Lichtenthaler [46].

4.5. Measurement of Total Nitrogen and Carbon

Additional leaf discs from where photosynthetic measurements were conducted were used for measurements of leaf carbon (C) and nitrogen (N) content. Leaf discs (0.353 cm^2) were oven-dried at 80 °C, weighed, and then ground to powder in a ball mill. Percentage of N and C was determined on the ground tissues using an Isoprime isotope-ratio mass spectrometer (Elementar).

4.6. Statistical Analyses

All statistical analyses were completed in GraphPad Prism™ 9.2.0 (GraphPad Software, San Diego, CA, USA). Where two-way ANOVA results were significant, a Tukey's multiple comparisons test was used to identify significant pair-wise differences arising from CO_2 treatment or plant genotype. p-values < 0.05 were considered significant.

Author Contributions: R.Y.Z. conducted physiology and biochemistry experiments, analysed data and wrote the manuscript. B.M. conducted biochemistry experiments, U.M. contributed resources and facilities and edited the manuscript, V.C.C. conceived the study, conducted physiology experiments, analysed data and edited the manuscript. All authors have read and agreed to the published version of the manuscript.

Funding: This research received no external funding.

Data Availability Statement: All raw data for this study is available online as supplementary data and includes uncropped western blots, raw data for CO_2 response curves, CABP assays, chlorophyll content and C and N analysis.

Acknowledgments: We are grateful to Hilary Stuart-Williams for his expertise and analysis of carbon and nitrogen in our samples, and to Susanne von Caemmerer for providing laboratory resources and sharing her photosynthetic expertise with us. We thank Julia Frugoli and Giles Oldroyd for the super-nodulating and non-nodulating mutants, respectively.

Conflicts of Interest: The authors declare no conflict of interest.

References

1. IPCC. Climate Change 2022: Mitigation of Climate Change. In *Contribution of Working Group III to the Sixth Assessment Report of the Intergovernmental Panel on Climate Change*; Shukla, P.R., Skea, J., Slade, R., Al Khourdajie, A., van Diemen, R., McCollum, D., Pathak, M., Some, S., Vyas, P., Fradera, R., et al., Eds.; Cambridge University Press: Cambridge, UK; New York, NY, USA, 2022.
2. Singer, S.D.; Chatterton, S.; Soolanayakanahally, R.Y.; Subedi, U.; Chen, G.; Acharya, S.N. Potential effects of a high CO_2 future on leguminous species. *Plant-Environ. Interact.* **2020**, *1*, 67–94. [CrossRef]
3. Ainsworth, E.A.; Long, S.P. What have we learned from 15 years of free-air CO_2 enrichment (FACE)? A meta-analytic review of the responses of photosynthesis, canopy properties and plant production to rising CO_2. *New Phytol.* **2005**, *165*, 351–372. [PubMed]
4. Kant, S.; Seneweera, S.; Rodin, J.; Materne, M.; Burch, D.; Rothstein, S.J.; Spangenberg, G. Improving yield potential in crops under elevated CO_2: Integrating the photosynthetic and nitrogen utilization efficiencies. *Front. Plant Sci.* **2012**, *3*, 162. [CrossRef] [PubMed]
5. Leakey, A.; Ainsworth, E.A.; Bernacchi, C.; Rogers, A.; Long, S.; Ort, D.R. Elevated CO_2 effects on plant carbon, nitrogen, and water relations: Six important lessons from FACE. *J. Exp. Bot.* **2009**, *60*, 2859–2876. [CrossRef] [PubMed]
6. Tausz, M.; Tausz-Posch, S.; Norton, R.M.; Fitzgerald, G.J.; Nicolas, M.E.; Seneweera, S. Understanding crop physiology to select breeding targets and improve crop management under increasing atmospheric CO_2 concentrations. *Environ. Exp. Bot.* **2013**, *88*, 71–80. [CrossRef]
7. Sulieman, S.; Thao, N.P.; Tran, L.-S.P. Does elevated CO_2 provide real benefits for N2-fixing leguminous symbioses? In *Legume Nitrogen Fixation in a Changing Environment*; Sulieman, S., Tran, L.-S.P., Eds.; Springer International Publishing: New York, NY, USA, 2015.

8. Reich, P.B.; Tilman, D.; Craine, J.; Ellsworth, D.; Tjoelker, M.G.; Knops, J.; Wedin, D.; Naeem, S.; Bahauddin, D.; Goth, J.; et al. Do species and functional groups differ in acquisition and use of C, N and water under varying atmospheric CO_2 and N availability regimes? A field test with 16 grassland species. *New Phytol.* **2001**, *150*, 435–448.
9. Lee, T.D.; Tjoelker, M.; Reich, P.; Russelle, M.P. Contrasting growth response of an N2-fixing and non-fixing forb to elevated CO_2: Dependence on soil N supply. *Plant Soil* **2003**, *255*, 475–486. [CrossRef]
10. Roy, S.; Liu, W.; Nandety, R.S.; Crook, A.D.; Mysore, K.S.; Pislariu, C.I.; Frugoli, J.A.; Dickstein, R.; Udvardi, M.K. Celebrating 20 Years of Genetic Discoveries in Legume Nodulation and Symbiotic Nitrogen Fixation. *Plant Cell* **2020**, *32*, 15–41. [CrossRef]
11. Udvardi, M.; Poole, P.S. Transport and Metabolism in Legume-Rhizobia Symbioses. *Annu. Rev. Plant Biol.* **2013**, *64*, 781–805. [CrossRef]
12. Cabrerizo, P.M.; González, E.M.; Aparicio-Tejo, P.M.; Arrese-Igor, C. Continuous CO_2 enrichment leads to increased nodule biomass, carbon availability to nodules and activity of carbon-metabolising enzymes but does not enhance specific nitrogen fixation in pea. *Physiol. Plant.* **2001**, *113*, 33–40. [CrossRef]
13. Fischinger, S.A.; Hristozkova, M.; Mainassara, Z.-A.; Schulze, J. Elevated CO_2 concentration around alfalfa nodules increases N2 fixation. *J. Exp. Bot.* **2010**, *61*, 121–130. [CrossRef]
14. Lüscher, A.; Hartwig, U.A.; Suter, D.; Nösberger, J. Direct evidence that symbiotic N_2 fixation in fertile grassland is an important trait for a strong response of plants to elevated atmospheric CO_2. *Glob. Chang. Biol.* **2000**, *6*, 655–662. [CrossRef]
15. Nakamura, T.; Koike, T.; Lei, T.; Ohashi, K.; Shinano, T.; Tadano, T. The Effect of CO_2 Enrichment on the Growth of Nodulated and Non-Nodulated Isogenic Types of Soybean Raised Under Two Nitrogen Concentrations. *Photosynthetica* **1999**, *37*, 61–70. [CrossRef]
16. Evans, J.R.; Clarke, V.C. The nitrogen cost of photosynthesis. *J. Exp. Bot.* **2019**, *70*, 7–15. [CrossRef] [PubMed]
17. Schulze, J.; Beschow, H.; Adgo, E.; Merbach, W. Efficiency of N2 fixation in *Vicia faba* L. in combination with different Rhizobium leguminosarum strains. *J. Plant Nutr. Soil Sci.* **2000**, *163*, 367–373.
18. Vance, C.P.; Heichel, G.C. Carbon in N2 fixation: Limitation or exquiste adaptation? *Annu. Rev. Plant Physiol. Plant Mol. Biol.* **1991**, *42*, 373–392. [CrossRef]
19. Ferguson, B.J.; Mens, C.; Hastwell, A.H.; Zhang, M.; Su, H.; Jones, C.H.; Chu, X.; Gresshoff, P.M. Legume nodulation: The host controls the party. *Plant Cell Environ.* **2019**, *42*, 41–51. [CrossRef] [PubMed]
20. Schnabel, E.L.; Kassaw, T.K.; Smith, L.S.; Marsh, J.F.; Oldroyd, G.E.; Long, S.R.; Frugoli, J.A. The ROOT DETERMINED NODULATION1 gene regulates nodule number in roots of Medicago truncatula and defines a highly conserved, uncharacterized plant gene family. *Plant Physiol.* **2011**, *157*, 328–340. [CrossRef]
21. Okamoto, S.; Shinohara, H.; Mori, T.; Matsubayashi, Y.; Kawaguchi, M. Root-derived CLE glycopeptides control nodulation by direct binding to HAR1 receptor kinase. *Nat. Commun.* **2013**, *4*, 2191. [CrossRef] [PubMed]
22. Nowak, S.; Schnabel, E.; Frugoli, J. The Medicago truncatula CLAVATA3-LIKE CLE12/13 signaling peptides regulate nodule number depending on the CORYNE but not the COMPACT ROOT ARCHITECTURE2 receptor. *Plant Signal. Behav.* **2019**, *14*, 1598730. [CrossRef]
23. Mortier, V.; Herder, G.D.; Whitford, R.; Van de Velde, W.; Rombauts, S.; D'Haeseleer, K.; Holsters, M.; Goormachtig, S. CLE Peptides Control Medicago truncatula Nodulation Locally and Systemically. *Plant Physiol.* **2010**, *153*, 222–237. [CrossRef] [PubMed]
24. Kassaw, T.; Nowak, S.; Schnabel, E.; Frugoli, J. ROOT DETERMINED NODULATION1 Is Required for M. truncatula CLE12, But Not CLE13, Peptide Signaling through the SUNN Receptor Kinase. *Plant Physiol.* **2017**, *174*, 2445–2456. [CrossRef] [PubMed]
25. Schnabel, E.; Journet, E.-P.; de Carvalho-Niebel, F.; Duc, G.; Frugoli, J. The Medicago truncatula SUNN Gene Encodes a CLV1-like Leucine-rich Repeat Receptor Kinase that Regulates Nodule Number and Root Length. *Plant Mol. Biol.* **2005**, *58*, 809–822. [CrossRef] [PubMed]
26. Goh, C.; Nicotra, A.B.; Mathesius, U. Genes controlling legume nodule numbers affect phenotypic plasticity responses to nitrogen in the presence and absence of rhizobia. *Plant Cell Environ.* **2019**, *42*, 1747–1757. [CrossRef]
27. Novák, K. On the efficiency of legume supernodulating mutants. *Ann. Appl. Biol.* **2010**, *157*, 321–342. [CrossRef]
28. Ben Amor, B.; Shaw, S.; Oldroyd, G.E.D.; Maillet, F.; Penmetsa, R.V.; Cook, D.; Long, S.R.; Dénarié, J.; Gough, C. The NFP locus of Medicago truncatula controls an early step of Nod factor signal transduction upstream of a rapid calcium flux and root hair deformation. *Plant J.* **2003**, *34*, 495–506. [CrossRef]
29. Jin, J.; Watt, M.; Mathesius, U. The Autoregulation Gene SUNN Mediates Changes in Root Organ Formation in Response to Nitrogen through Alteration of Shoot-to-Root Auxin Transport. *Plant Physiol.* **2012**, *159*, 489–500. [CrossRef]
30. Qiao, Y.; Miao, S.; Jin, J.; Mathesius, U.; Tang, C. Differential responses of the sunn4 and rdn1-1 super-nodulation mutants of Medicago truncatula to elevated atmospheric CO_2. *Ann. Bot.* **2021**, *128*, 441–452. [CrossRef]
31. Ermakova, M.; Lopez-Calcagno, P.E.; Raines, C.A.; Furbank, R.T.; von Caemmerer, S. Overexpression of the Rieske FeS protein of the Cytochrome b6f complex increases C4 photosynthesis in Setaria viridis. *Commun. Biol.* **2019**, *2*, 314. [CrossRef]
32. Simkin, A.J.; McAusland, L.; Lawson, T.; Raines, C.A. Overexpression of the RieskeFeS Protein Increases Electron Transport Rates and Biomass Yield. *Plant Physiol.* **2017**, *175*, 134–145. [CrossRef]
33. Parry, M.A.J.; Andralojc, P.J.; Mitchell, R.; Madgwick, P.J.; Keys, A.J. Manipulation of Rubisco: The amount, activity, function and regulation. *J. Exp. Bot.* **2003**, *54*, 1321–1333. [CrossRef]

34. Zheng, Y.; Li, F.; Hao, L.; Yu, J.; Guo, L.; Zhou, H.; Ma, C.; Zhang, X.; Xu, M. Elevated CO_2 concentration induces photosynthetic down-regulation with changes in leaf structure, non-structural carbohydrates and nitrogen content of soybean. *BMC Plant Biol.* **2019**, *19*, 255. [CrossRef] [PubMed]
35. Wang, J.; Liu, X.; Zhang, X.; Li, L.; Lam, S.K.; Pan, G. Changes in plant C, N and P ratios under elevated [CO_2] and canopy warming in a rice-winter wheat rotation system. *Sci. Rep.* **2019**, *9*, 5424. [CrossRef]
36. Hansen, A.P.; Gresshoff, P.M.; Pate, J.S.; Day, D.A. Interactions between Irradiance Levels, Nodulation and Nitrogenase Activity of Soybean cv. Bragg and a Supernodulating Mutant. *J. Plant Physiol.* **1990**, *136*, 172–179. [CrossRef]
37. Becanamwo, M.; Harper, J. Response of a hypernodulating soybean mutant to increased photosynthate supply. *Plant Sci.* **1997**, *124*, 119–129. [CrossRef]
38. Ainsworth, E.A.; Davey, P.A.; Bernacchi, C.J.; Dermody, O.C.; Heaton, E.A.; Moore, D.J.; Morgan, P.B.; Naidu, S.L.; Yoo Ra, H.S.; Zhu, X.G.; et al. A meta-analysis of elevated [CO_2] effects on soybean (Glycine max) physiology, growth and yield. *Glob. Chang. Biol.* **2002**, *8*, 695–709. [CrossRef]
39. Singh, S.K.; Barnaby, J.; Reddy, V.R.; Sicher, R.C. Varying Response of the Concentration and Yield of Soybean Seed Mineral Elements, Carbohydrates, Organic Acids, Amino Acids, Protein, and Oil to Phosphorus Starvation and CO_2 Enrichment. *Front. Plant Sci.* **2016**, *7*, 1967. [CrossRef]
40. Li, Y.; Yu, Z.; Jin, J.; Zhang, Q.; Wang, G.; Liu, C.; Wu, J.; Wang, C.; Liu, X. Impact of Elevated CO_2 on Seed Quality of Soybean at the Fresh Edible and Mature Stages. *Front. Plant Sci.* **2018**, *9*, 1413. [CrossRef] [PubMed]
41. Unkovich, M.; Herridge, D.; Peoples, M.; Cadisch, G.; Boddey, R.; Giller, K.; Alves, B.; Chalk, P. *Measuring Plant-Associated Nitrogen Fixation in Agricultural Systems*; ACIAR Monograph No. 136: Canberra, Australia, 2008; 258p.
42. Bergersen, F. The growth of rhizobium in synthetic media. *Aust. J. Biol. Sci.* **1961**, *14*, 349. [CrossRef]
43. Schneider, C.A.; Rasband, W.S.; Eliceiri, K.W. NIH Image to ImageJ: 25 Years of image analysis. *Nat. Methods* **2012**, *9*, 671–675. [CrossRef]
44. Sharkey, T.D.; Bernacchi, C.J.; Farquhar, G.D.; Singsaas, E.L. Fitting photosynthetic carbon dioxide response curves for C_3 leaves. *Plant Cell Environ.* **2007**, *30*, 1035–1040. [CrossRef] [PubMed]
45. Ruuska, S.; Andrews, T.J.; Badger, M.R.; Hudson, G.S.; Laisk, A.; Price, G.D.; Von Caemmerer, S. The interplay between limiting processes in C3 photosynthesis studied by rapid-response gas exchange using transgenic tobacco impaired in photosynthesis. *Funct. Plant Biol.* **1998**, *25*, 859–870. [CrossRef]
46. Lichtenthaler, H.K. Chapter 34. Chlorophylls and carotenoids: Pigments of photosynthetic biomembranes. *Methods Enzymol.* **1987**, *148*, 350–382.

Disclaimer/Publisher's Note: The statements, opinions and data contained in all publications are solely those of the individual author(s) and contributor(s) and not of MDPI and/or the editor(s). MDPI and/or the editor(s) disclaim responsibility for any injury to people or property resulting from any ideas, methods, instructions or products referred to in the content.